Mathematical models for error correction in MScMS-II (Mobile Spatial coordinate Measurement System)

MATHEMATICAL MODELS FOR ERROR CORRECTION IN MScMS-II (MOBILE SPATIAL COORDINATE MEASUREMENT SYSTEM)

GALETTO MAURIZIO, MASTROGIACOMO LUCA

DIGEP- Politecnico di Torino, C.so Duca degli Abruzzi 24, Torino, 10129, Italy
e-mail: maurizio.galetto@polito.it

This paper presents three mathematical models for the correction of measurement errors of a prototype system designed for Large Scale Dimensional Metrology (LSDM) applications. The system, developed in the Quality and Industrial Metrology Laboratory of Politecnico di Torino, is based on the principles of photogrammetry and consist of a set of cameras wirelessly connected to a central unit for data elaboration and able to track the position of a hand-held contact probe. Due to its architecture the system is affected by several systematic error sources. This paper addresses some of them: the distortion of the lenses, the dimension of the probe tip and the kinematic of the probe. By means of the implementation of appropriate mathematical correction models, the overall system performance is significantly improved as shown by the proposed tests.

Keywords**:** *MScMS-II, Large Scale Dimensional Metrology, error correction.*

1. Introduction To The Problem

Nowadays, one of the most challenging issues in Large Scale Dimensional Metrology (LSDM) applications is to ensure consistent instrument performance throughout the whole working volume. Distributed measurement systems, which are based on a network of metrology stations spread in a well defined working volume, particularly suffer this problem. Several corrective models have been proposed in order to partially address this issue. Some of them are already integrated into the onboard firmware and software applications [1,2]. This paper deals with the mathematical models for error correction implemented into a new prototype system developed at Politecnico di Torino, the Mobile Spatial coordinate Measurement System (MScMS-II) [2].

Relying on the principles of close-range photogrammetry, MScMS-II is characterized by a distributed modular architecture, consisting of a network of wireless sensing devices, a remote hand-held and armless probe, and a centralized data processing unit (DPU) (Figure 1) [2]. The network consists of a set of IR cameras, that communicate to the DPU, through a wireless Bluetooth link, the information related to the spatial positioning of two reference markers mounted on the hand-held probe. Low-cost IR cameras, characterized by an interpolated resolution of 1024x768 pixels, a maximum sample rate of 100 Hz, and an angular Field-Of-View (FOV) of approximately 45°×30°, have been chosen as sensor network devices [4]. The position and orientation of each camera is defined by a specific calibration procedure performed just before the measurement process [2,5]. Since passive tracking has been implemented, each sensor is coupled with a near-IR light source (IR LED array, see Figure 1) to properly floodlight the working volume and hence possible retro-reflective markers visible in the camera field-of-sensing. Each camera is provided with an embedded real-time tracking engine, which is in charge of image processing and filtering and determines the 2D coordinates of the IR spot(s) in the camera view plane [3,4].

The DPU processes the data acquired from each sensing device and elaborates them to provide 3D coordinates of the probe tip (V).

In the paper, three different kind of systematic effects – respectively due to the lens distortion, the probe physical size and its kinematic during measurement – are analyzed. All the evaluation tests of the effect of each correction are performed within the MScMS-II prototype layout of 3x3x2 m^3.

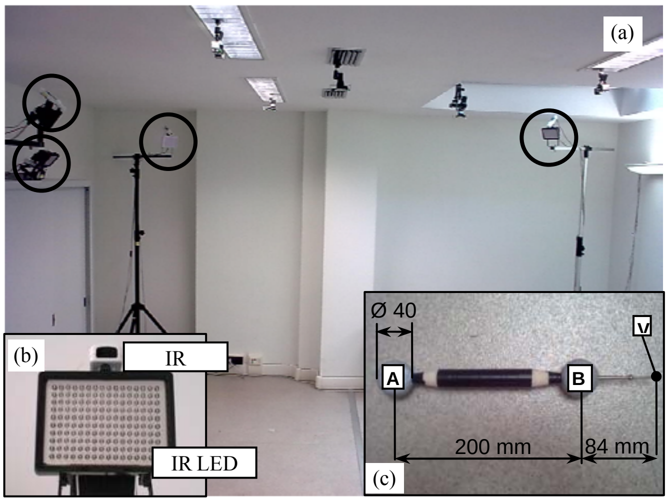

Figure 1. MScMS-II prototype [2]. (a) Sensor network configuration: black circles highlight the spatial position of the network nodes. (b) Main components of the IR-based sensor network. (c) Portable hand-held probe.

2. Lens Distortion

Lens distortion constitutes the major imaging error for most camera systems. It can be modeled as the sum of two components: radial and tangential distortion [3]. Radial distortion is attributable to variations in refraction at each individual component lens within the objective, while tangential distortion is mainly caused by decentring and misalignment of individual lens elements within the objective. The complete correction model can be stated as:

$$u_{corrected} = u + [u(k_1 r^2 + k_2 r^4 + k_3 r^6 + ...)]_{rad} + [b_1 (r^2 + 2u^2) + 2b_2 uv]_{tg}$$
$$v_{corrected} = v + [v(k_1 r^2 + k_2 r^4 + k_3 r^6 + ...)]_{rad} + [b_2 (r^2 + 2v^2) + 2b_1 uv]_{tg}$$

where u, v are the normalized pixel coordinates of a camera, $r = \sqrt{u^2 + v^2}$ is the radial coordinate, k_1 *to* k_n and b_1, b_2 are respectively the radial and tangential distortion coefficient.

2.1. *Test*

In order to verify the effectiveness of the proposed model, the following test was made [6]. A reference artifact was calibrated using a Coordinate Measuring Machine (CMM – DEA Iota 0101). On the artifact four different reference distances of about 100, 200, 400 and 500 mm were defined. The reference artifact was then moved in three different positions within the measuring volume of MScMS-II. For each position of the reference artifact, the distances were measured with MScMS-II, replicating the measurements 10 times (for a total of 4·3·10=120 measurements).

The results of these measurements with and without the correction of lens distortion were compared in terms of deviation from nominal values. In order to quantify the improvement, Table 1 shows the sample mean and the standard deviation of the error distribution with and without the correction model.

Table 1. Sample mean and standard deviation of error distribution.

	Without Correction	With Correction
Mean [mm]	-0.57	0.09
Standard deviation [mm]	1.61	0.82

As expected, the performance of the system seems to improve with the distortion correction. The improvement is significant both in terms of bias and in terms of dispersion of the error distribution.

In order to verify the robustness of the obtained results, the test has been repeated with the same and with different network layouts (i.e. with different position and orientation of the IR cameras), producing comparable results.

3. Bias Due To The Physical Size Of The Probe

A common problem to all contact measuring instruments is the size of the tip of the probe which may introduce a bias in the contact measurement [1]. For this reason, CMMs software typically implement some algorithms able to correct the measurement results taking into consideration the direction of the approach of the probe and the surface shape to be measured (see Figure 2) [1,7].

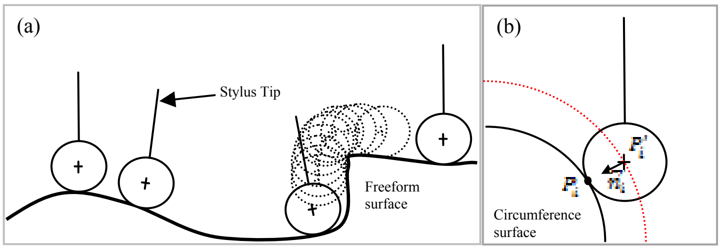

Figure 2. A schematization of the stylus tip approach to a freeform (a) and a circumference (b). The dotted line in (b) represents the envelope of the points measured by the CMM which, in this particular case, corresponds to a circumference with a greater radius.

The stylus tip radius correction (see Figure 2) is an offset vector of norm equal to the effective stylus tip radius which is added to the indicated measured point (i.e. the measured stylus tip centre point) to estimate the actual contact or measured point on the profile (i.e. the stylus tip actual contact point on the real surface). The nature of the tangential contact between a sphere and a surface results in the offset vector being normal to the surface at the point of contact so the primary task for correction is to estimate this vector for each data point. In the case of a freeform surface or for a contour, the measuring surface normal vector is unknown. A number of approaches have been proposed for solving this problem [7]. Without going into details of the case of freeform surfaces which is widely debated in the literature, the purpose of this section is to describe the technical implementation of error compensation in case of areas sections of a known geometric primitive such as a plane, circle, sphere, cone, torus, etc., analyzing the effects of such implementation on MScMS-II.

With MScMS-II, this correction is negligible using a sharp tip. This type of probe, however, has several drawbacks that limit its use: it is not able to make measurements approaching the piece sideways; it may introduce a geometrical error due to the imperfections of the tip; it introduce a risk of damage to the object to be measured.

3.1. *Implementation Of The Correction*

From the practical point of view, the procedure implemented for MScMS-II can be summarized in the following steps (see Figure 2):

1. Specification of the target geometry. During this phase the system user is asked to specify the geometry of the surface to be measured.
2. Measurement. In this phase a certain number of points P'_i is acquired by means of the hand-held probe.
3. Reconstruction of the envelop. Knowing the specified geometry of the surface, the system computes the envelop which interpolates the points P'_i.
4. Calculation of the touched points. Knowing the radius of the tip of the probe, the position of the center of the probe P'_i and the surface normal $\vec{n}_i$, the generic contact point P'_i can be obtained through the relation:

$$P_i = P'_i \pm \vec{n}_i \cdot \rho.$$

The sign of the sum depends on the direction of approach of the probe.

As an example, consider the simple case of estimating a two-dimensional geometry: a circumference. When measuring a circumference, the envelope of points corresponds with another circle, with the same center but different radius. The radius depends on the measurement procedure: if the measurement is made approaching the circumference from the outside (case of a shaft) the radius will be greater than the real one (see Figure 2(b)) and vice versa if the measurement is made from within (case of a hole).

During the third step of the procedure described above, the system is able to calculate the geometry of the envelope points P'_i. For example, in case of a circumference measured from the outside (see Figure 2(b)), the radius ρ' and the center x_0 of the envelope are calculated.

So far, for each point of the envelop, the normal vector is:

$$\vec{n} = \frac{x_0 - P_i}{\rho}.$$

Knowing the normal vector, the contact points P'_i can be calculated as $P_i = P'_i + \vec{n}_i \cdot \rho$. Note the positive sign of the equation. It would have been negative in case of a measurement made with the probe approaching from the inside.

3.2. *Test*

To make explicit the extent of the improvement deriving from the implementation of the correction model described above, the following test was designed. A section of a cylinder calibrated by a CMM (DEA Iota 0101) was measured with MScMS-II for which the exact probe radius correction is known. The measurement was repeated 30 times in different locations within the working volume of MScMS-II.

The results of the measurements with and without correction model were compared with each other. If compared to the nominal value of the diameter of the cylinder section (d = 120 mm), the results show an average bias in the measurement of b = 0.98 mm, that, as expected, is about half the size of the tip of MScMS-II probe (2 mm). This average bias reduces to 0.02 mm when the measurement is corrected considering the size of the probe tip.

The proposed test was conducted on a section of the cylinder for practical reasons. It is reasonable to expect similar results when the surface to be measured is a free form. In this case, however, complications may arise from the need to calculate a point by point estimation of the surface normal vector.

4. Bias Due To The Kinematic Of The Probe

When measuring using the MScMS-II, the operator has to bring the probe in contact with the object being measured. At this point, he presses a trigger to take measurements [2]. Although fast enough, this operation is not instantaneous. When the trigger is pressed, the system collects a sample of measurement replications for a fraction of a second (less than one third of a second). During this period, the position of the tip of the probe is supposed to be stationary. For this reasons, the process may be modeled over time as [8]:

$$x_k = x_{k-1} + w_k,$$

with a measurement $z \in \mathbb{R}^3$ that is

$$z_k = x_k + v_k,$$

where $x_k \in \mathbb{R}^3$ is the position of the probe tip at time k and the random variables $w_k \in \mathbb{R}^3$ and $v_k \in \mathbb{R}^3$ represent the process and measurement noise. They are assumed to be independent (of each other), white, and with normal probability distributions, i.e. $p(w) \sim N_3(0, Q)$ and $p(v) \sim N_3(0, R)$. Q and R are respectively the process noise covariance and the measurement noise covariance matrices. Although they could potentially vary in time, they are assumed to be constant in time.

4.1. *The Kalman Filter*

The Kalman filter is essentially a set of mathematical equations that implement a predictor-corrector type estimator that is optimal in the sense that it minimizes the estimated error covariance when some presumed conditions are met [8]. One of the assumptions for the application of the Kalman filter is the knowledge of the measurement process.

4.2. *The Filter Equation Parameters*

The time update equations are

$$\hat{x}_k^- = \hat{x}_{k-1}^-$$
$$P_k^- = P_{k-1}^- + Q,$$

where P_k^- and P_{k-1}^- are respectively the *a priori* estimates of error covariance at time step *k* and *k-1* and $\hat{x}_k^-$ and $\hat{x}_{k-1}^-$ are respectively the *a priori* state estimates at time step *k* and *k-1*.

On the other hand, the measurement update equations are

$$K_k = P_k^-(P_k^- + R)^{-1}$$
$$\hat{x}_k = \hat{x}_k^- + K_k(z_k - \hat{x}_k^-)$$
$$P_k = (1 - K_k)P_k^-,$$

Where P_k is the *a posteriori* estimate of error covariance, $\hat{x}_k$ is the *a posteriori* state estimate at time step *k*, K_k is the gain that minimizes the *a posteriori* error covariance at step *k* [8].
Presuming a very small process variance, it is possible to assume

$$Q = \begin{pmatrix} 1e^{-5} & 0 & 0 \\ 0 & 1e^{-5} & 0 \\ 0 & 0 & 1e^{-5} \end{pmatrix}.$$

Assuming a small but non-zero value for Q gives more flexibility in "tuning" the filter [8]. The filter is "seed" with the guess $\hat{x}_{k-1}^- = x_0$. Similarly the initial value for P_{k-1}, call it P_0 as well as the measurement error variance *R* are set as the Identity matrix [8].

4.3. *Test*

In normal operation conditions, the measurement of the position of the probe tip is the result of the acquisition of approximately thirty repetitions of measurement. The system, in fact, has a capture rate that ensures, under these assumptions, an acquisition time of less than 3 tenths of a second. During this period the operator is supposed to keep the probe tip reasonably still.

To give evidence of the effect of the implementation of the filter, 300 repetitions of measurement have been recorded keeping the probe still for about 3 seconds. There is evidence of the fact that the filtered measurements are much more stable than the unfiltered ones. Considering the first 30 observations, the standard deviations of filtered data are respectively $\sigma_x = 0.07$ mm, $\sigma_y = 0.04$ mm and $\sigma_z = 0.09$ mm. On the other hand, the standard deviations of unfiltered data are respectively $\sigma_x = 0.35$ mm, $\sigma_y = 0.13$ mm and $\sigma_z = 0.29$ mm.

5. Conclusions And Future Developments

This work stems from the need to address three open problems in the development of MScMS-II: the error due to lens distortion and the bias due to both the physical size of the probe and its kinematic. Although the paper addresses the issues in depth with satisfactory results, this study opens several research scenarios for the improvement of the system. As regards the model of lens distortion, a thorough study should be carried out in order to investigate the contributions of the various terms of the polynomial correction. The questions, in this case would be: “In what order is it worth truncating the polynomial development of the model? And which are the effects of the calibration procedure on the calculation of the coefficients of the polynomial?”. On the other hand, the study of the kinematic of the probe led to the introduction of the Kalman filter to filter the noise that the instrument introduces to the static measurement. The natural extension of the model to kinematic tracking has still to be considered and analyzed.

6. References

1. J.A. Bosch, *Coordinate Measuring Machines and Systems*. New York: Marcel Dekker Inc. (1995).
2. F. Franceschini, M. Galetto, D.A. Maisano, L. Mastrogiacomo, B. Pralio, *Distributed Large-Scale Dimensional Metrology*. *New Insights*. London: Springer Verlag London Ltd. (2011).
3. T. Luhmann, S. Robson, S. Kyle, I. Harley, *Close-Range Photogrammetry: Principles. Techniques and Applications*. New York: John Wiley & Sons Inc. (2007).
4. J.C. Lee, *Hacking the Nintendo Wii Remote*. IEEE Pervasive Computing 7(3):39–45 (2008).
5. D.C. Brown, *Close-range camera calibration*. Photogrammetric Engineering, 37(8):855-866 (1971).
6. VDI/VDE 2634-1/2/3, *Optical 3D measuring systems. Part 1: Imaging systems with point-by-point probing – Part 2: Optical systems based on area scanning – Part 3: Multiple view systems based on area scanning*. Berlin: Beuth Verlag GmbH (2002, 2002, 2008).
7. A. Woźniak, *Stylus tip envelop method: corrected measured point determination in high definition coordinate metrology*. International Journal of Advanced Manufacturing Technology, 42:505–514 (2009).
8. Y. Bar-Shalom, X.R. Li, T. Kirubarajan, Estimation with applications to tracking and Navigation. New York: John Wiley & Sons Inc. (2001).